NJC
New Journal of Chemistry
A journal for new directions in chemistry

Accepted Manuscript

This article can be cited before page numbers have been issued, to do this please use: S. brahma, R. Borah and N. Deori, *New J. Chem.*, 2020, DOI: 10.1039/C9NJ04606B.

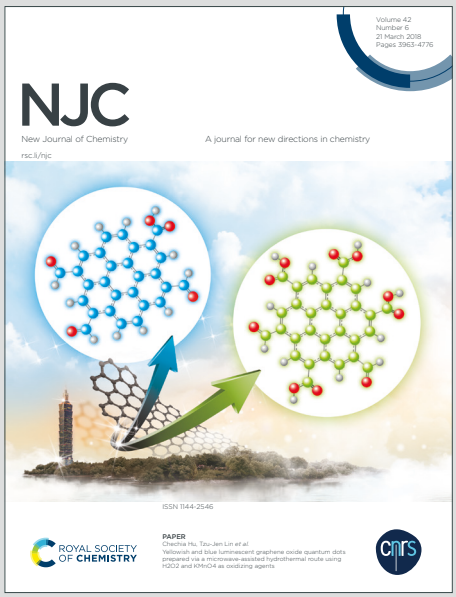

This is an Accepted Manuscript, which has been through the Royal Society of Chemistry peer review process and has been accepted for publication.

Accepted Manuscripts are published online shortly after acceptance, before technical editing, formatting and proof reading. Using this free service, authors can make their results available to the community, in citable form, before we publish the edited article. We will replace this Accepted Manuscript with the edited and formatted Advance Article as soon as it is available.

You can find more information about Accepted Manuscripts in the Information for Authors.

Please note that technical editing may introduce minor changes to the text and/or graphics, which may alter content. The journal's standard Terms & Conditions and the Ethical guidelines still apply. In no event shall the Royal Society of Chemistry be held responsible for any errors or omissions in this Accepted Manuscript or any consequences arising from the use of any information it contains.

View Article Online
DOI: 10.1039/C9NJ04606B

ARTICLE

,Received 00th January 20xx,
Accepted 00th January 20xx
DOI: 10.1039/x0xx00000x

An efficient CO_2 fixation reaction with epoxides catalysed by *in situ* formed blue vanadium catalyst from dioxovanadium(+5) complex: Moisture enhanced and atmospheric oxygen retarded catalytic activity

Rakhimoni Borah,[a] Naranarayan Deori,[a] Sanfaori Brahma*[a]

Abstract: Two new dioxovanadium(+5) complexes, one anionic and other neutral, have been synthesised and X-ray crystallographically characterised here in this work. While doing cycloaddition reaction of CO_2 to epoxides taking dioxovanadium(+5) complex as catalyst, a blue vanadium complex was generated *in situ* which is found to be the active catalyst, showing excellent catalytic activity in presence of tetrabutyl ammonium bromide as co-catalyst. The catalytic activity of the catalyst system is enhanced by moisture, on the other hand, retarded by atmospheric oxygen. The enhanced catalytic activity at moistened condition shows the applicability of the catalyst for the CO_2 fixation from wet flue gas. However, retarded catalytic activity caused by atmospheric oxygen is important from the mechanistic point of view.

1 Introduction

Chemical fixation of CO_2 can be considered as the most effective greener approach, which paved a way for better employment of carbon resources thereby fulfilling the need for sustainable development. CO_2 is inexpensive, non-toxic, easy to handle and largely available from fossil fuel combustion. Also, utilization of CO_2 in producing cyclic carbonates is a highly significant one, since chemically important cyclic carbonates can be obtained from greenhouse gas CO_2.[1-25] Cyclic carbonates can serve as an excellent polar aprotic solvent[26] and electrolytes in lithium ion batteries.[27, 28] They are also valuable raw materials for synthesizing polyurethanes,[29] polycarbonates,[30, 31] polyglycerol[32] and small molecules such as dimethylcarbonate.[33] Moreover, carbonate moiety is seen in natural products.[34-36] Keeping in view the importance of the above said reaction, numerous catalyst systems have been so far developed which aims at increasing the reaction efficiency by minimizing the harsh reaction conditions. These potential catalytic systems include various transition metal-based catalysts such as metal-salen or salphen,[37-41] metal-porphyrin,[42-46] and metal organic frameworks (MOF)[47-50] and on the other hand organocatalysts[51-57] like Schiff base,[54] quaternary ammonium or phosphonium salts,[55, 56] and ionic liquids (ILs).[57] As compared to other transition metals, vanadium is not much exploited for this type of incorporation of carbon dioxide to epoxides. Although there are many examples of oxo and dioxovanadium complexes bearing tridentate hydrazine based ligands[58-72] which are investigated for different purpose such as, to see their antimicrobial activity,[59] as catalyst in oxidation of various substrates,[60, 65] their use in cycloaddition reaction of CO_2 to epoxides are yet to be explored in detail. Specially, involvement of dioxovanadium(V) complex of salicylidene hydrazide ligands are very scarcely reported. Lee and co-workers reported that VCl_3 was able to carry out the catalytic reaction between epoxides and CO_2.[73] However, it required high temperatures (90-120 °C) and pressure (15 bar). Recently, excellent vanadium catalysts have been added to the library of catalysts for the reaction of various epoxides and CO_2 by the groups of Kerton,[11] Kleij[12, 23] and others.[45]

In this work, we have been able to synthesise two dioxovanadium(V) complexes of salicylidene hydrazide ligand, $[NH_4][VO_2(Sal\text{-}ac)]$, **1** and its analogous complex devoid of ammonium $[VO_2(HSal\text{-}ac)]$, **2**. It has been found that both the dioxovanadium complex **1** and **2** have efficient catalytic activity towards cycloaddition reaction of carbon dioxide with epoxides under mild reaction conditions. However, detailed catalytic studies were done by taking catalyst **1**, as it shows better catalytic efficacy compared to catalyst **2**.

2 Results and Discussion

2.1 Synthesis

Scheme 1 shows the synthetic route of the dioxovanadium(V) complexes $[NH_4][VO_2(Sal\text{-}ac)]$, **1** and $[VO_2(HSal\text{-}ac)]$, **2**. Ligand, N-(2-

[a] Department of Chemistry, Gauhati University
Guwahati-781014, Assam, India.
E-mail: sanfaoribrahma@gmail.com
† Supporting Information and ORCID identification number(s) for the author(s) of this article can be found under: https://doi.org/xxxxxx

View Article Online
DOI: 10.1039/C9NJ04606B

hydroxybenzylidene)acetohydrazide has been prepared by mixing salicylaldehyde and acetohydrazide in methanol and stirring the mixture for about half an hour till a pale yellow solid formed.[59] Yellow solid dioxovanadium(+5) complex, $[NH_4][VO_2(Sal\text{-}ac)]$, **1** has been obtained by refluxing the ligand with methanolic solution of ammonium metavanadate for about 8-10 hours after reducing the volume.[61] On the other hand, complex **2** was obtained by heating the dimethylformamide solution of the ligand with ammonium metavanadate at 80 °C for 5 hours.[62]

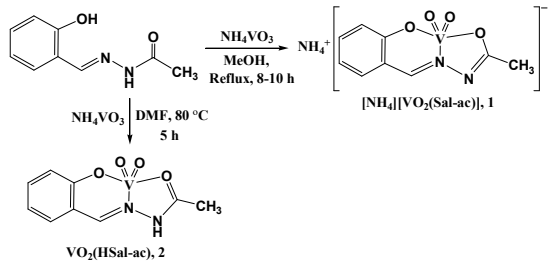

Scheme 1. Synthesis of $[NH_4][VO_2(Sal\text{-}ac)]$, **1** and $[VO_2(HSal\text{-}ac)]$, **2**.

2.2 ^{1}H NMR Spectra

^{1}H NMR spectrum reveals the formation of complex **1** (Fig. 1). It is note to be mentioned that resonance at 7.11 ppm is attributed to the counter cation NH_4^+ present in complex **1**.[63] However, in the ^{1}H NMR spectrum of complex **2** (Fig. S1†), no such peak is appeared implicating that there is no ammonium counter cation as indicated by the crystal structure. The ^{1}H NMR spectra of both the complexes show resonances at diamagnetic region indicating the complexes to be diamagnetic where vanadium is in +5 oxidation state.

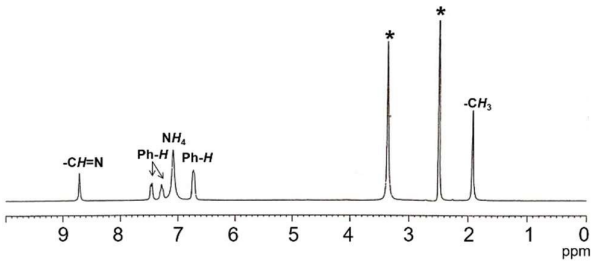

Fig. 1 ^{1}H NMR spectrum of $[NH_4][VO_2(Sal\text{-}ac)]$, **1** in $[D_6]$ DMSO (Asterisks represents solvent impurities of water in $[D_6]$ DMSO).

2.3 IR Spectra

The band due to ν(C=O) in the free ligand at 1683 cm^{-1} disappears in the infra-red spectrum of the complex **1**, suggesting enolization of the ligand and coordination of enol form of the ligand (Fig. S2†). A new band at 1282 cm^{-1} may be due to the enolic ν(C-O).[64] The observed band at 1614 cm^{-1} is ascribed to ν(C=N) of the azomethine group.[59] Two bands observed at 893 and 942 cm^{-1} are due to symmetric ν(O=V=O) and antisymmetric ν(O=V=O) stretches respectively.[65] The presence of these two intense bands confirms the formation of dioxo complex of vanadium. Similar stretching frequencies observed in the IR spectrum of the complex **2** confirm its formation (Fig. S3†).

2.4 UV/Vis Spectrum

UV/Vis spectrum of complex **1** depicted in Fig. S4† are also in accordance with the previously reported dioxovanadium complexes.[62, 65] Band at 219 nm appears due to π-π* transition, band at 293 nm corresponds to n–π* transition and band at 370 nm occurs due to LMCT between ligand and vanadium(+5) which overlaps with the band arised due to the extended conjugation in the ligand system.[64]

2.5 Crystallographic Characterization

Yellow block shaped crystals obtained by slow evaporation of solution containing complex **1** in methanol and acetonitrile mixture (1:3), has similar structural parameters with the previously reported ones (Fig. 2).[58-65] V-O1 and V-O2 distances are similar and are found to be 1.9714(19) and 1.893(2) Å respectively, however V-O3 and V-O4 distances are significantly shorter 1.619(2) and 1.646(2) Å, respectively implicating V=O nature of the bond. Crystal packing diagram, data collection parameters and the selected bond distances and angles are shown in Fig. S5†, Table S1 and Table S2, respectively.

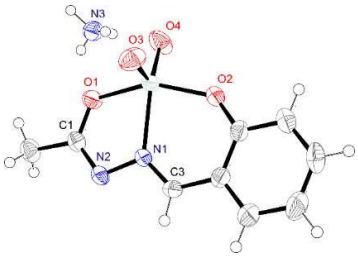

Fig. 2 A perspective view of **1** showing 50% thermal contours for all non-hydrogen atoms at 296(2) K. Selected bond distances (Å) and angles (°): for molecule **1**, V-O1, 1.9714(19); V-O2, 1.893(2); V–O3, 1.619(2); V–O4, 1.646(2); V-N1, 2.128(2); N1-N2, 1.406(3); N2-C1, 1.296(3); N1-C3, 1.297(4); O1-C1, 1.305(3); O(3)-V-O(4), 109.54(13); O(1)-V-O(2), 150.56(9).

Brownish needle shaped crystals obtained by slow evaporation of solution containing complex **2** in dimethylformamide and toluene solvent mixture, has similar structural parameters with the previously reported ones (Fig. 3).[58-65]

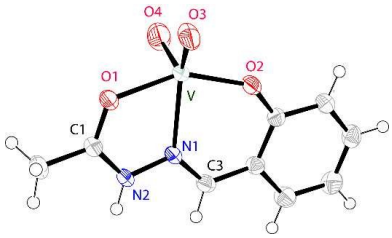

Fig. 3 A perspective view of **2** showing 50% thermal contours for all non-hydrogen atoms at 296(2) K. Selected bond distances (Å) and angles (°): for molecule **2**, V-O1, 2.0181(18); V-O2, 1.8742(17); V–O3, 1.6315(19); V–O4, 1.601(2); V-N1, 2.1682(19); N1-N2, 1.379(3); N2-C1, 1.312(3); N1-C3, 1.295(3); O1-C1, 1.260(3); O(3)-V(1)-O(4), 109.37(13); O(1)-V(1)-O(2), 150.81(8).

DOI: 10.1039/C9NJ04606B

As obtained in crystal structure of the complex **1**, similar bond distances are found in the crystal structure of the complex **2**. However, the V-O1 bond distance in complex **1** is shorter by 0.0467 Å than V-O1 bond length in complex **2**, as O1 makes a stronger bond with vanadium because of negative charge produced in O1 after its deprotonation which is not the case with O1 in complex **2**. Crystal packing diagram, data collection parameters and the selected bond distances and angles are shown in Fig. S6†, Table S1 and Table S2, respectively.

2.6 Catalytic Studies

Anionic dioxovanadium(V) catalyst, **1** has shown to be efficient catalyst for the cycloaddition reaction of CO_2 to epoxides resulting in the formation of corresponding cyclic carbonates (Table 1). Catalytic cycloaddition was performed by loading epoxide, catalyst **1** and co-catalyst tetrabutylammonium bromide (TBAB) in a stainless-steel autoclave equipped with a magnetic stirring bar and dosing appropriate pressure of CO_2. Formation of cyclic carbonate has been confirmed by the ^{1}H NMR (Fig. S7-S18†) and ^{13}C NMR (Fig. S19†) showing downfield shifting of the peaks compared to epoxide because of addition of CO_2. IR resonance at 1801 cm^{-1} also confirms the formation of cyclic carbonate (Fig. S20†).[74] Percentage conversions of epoxides to the cyclic carbonates are calculated with the help of ^{1}H NMR spectrum taken from the reaction mixture. Epichlorohydrin and styrene oxide were taken as substrates for the catalytic studies. To compare the catalytic efficiency of anionic catalyst **1** with neutral catalyst **2**, catalytic reactions were performed separately at 60 °C for 2 hours taking styrene oxide as substrate and was found that catalyst **1** gave better yield than **2** (entry 1 and 2). Therefore, catalyst **1** was considered for subsequent catalytic studies. When the catalytic reaction was performed using catalyst **1** at 45 °C and 5 bar pressure of CO_2 for 14 hours, epichlorohydrin showed 99 % conversion (entry 3), while styrene oxide resulted 83 % conversion (entry 4). Upon increasing the reaction temperature to 60 °C, 95 % conversion was observed at mere 4 hours (entry 5) for epichlorohydrin and 91 % for styrene oxide (entry 6). While, TBAB alone could result 40% conversion of epoxide to cyclic carbonate (entry 7), catalyst alone does not have any catalytic activity (entry 8), even when the reaction was done at 45 °C for 15 hours. To our surprise, it is found that moistened TBAB alone has enhanced catalytic capability compared to unmoistened TBAB, which becomes evident when an increase in the conversion from 24 % to 37 % (compare entry 9 and 10) was obtained for styrene oxide with moistened TBAB. A lesser conversion of 75% obtained when the reaction was carried out by using unmoistened TBAB along with catalyst compared to 91% conversion obtained by using moistened TBAB further supports our observation (compare entry 6 and 11). The plausible explanation for the enhanced catalytic capability of the moistened TBAB may be due to activation of epoxide by the H^+ released from the carbonic acid generated from CO_2 and moisture. It was observed that the reaction mixture which was initially yellow turns blue upon completion of the reaction.[23] This blue reaction mixture produced after the catalytic reaction can be attributed to the +4 oxidation state (*vide infra*) of vanadium generated during the reaction. To see the yield of the catalytic reaction, reaction mixture of styrene oxide and carbon dioxide (entry 6) was subjected to column chromatography. The yield of isolated styrene carbonate was found to be 86 %, while a conversion of 91 % was observed from ^{1}H NMR spectrum of the same reaction mixture, showing not much difference between the yield and conversion. Thus, we can say that cyclic carbonate is the sole product produced from epoxide. The ^{1}H NMR spectrum of the isolated styrene carbonate is shown in Fig. S18†.

Surprisingly, catalyst has lower activity indicated by lower conversion (60 %), when the reaction was conducted without flushing the atmospheric air present in reaction vessel with CO_2 gas (entry 12) compared to the 91 % conversion (entry 6) when the reaction was done by evacuating the vessel by CO_2 gas, keeping other reaction conditions same. It is to be mentioned that even after the reaction was performed for 4 hours at 60 °C without evacuating the atmospheric oxygen of reaction vessel by CO_2, the reaction mixture was only slightly blue (entry 12) which indicates that the oxygen present in the vessel set difficulty in the reduction of V(+5) to V(+4). This clearly suggests that the blue vanadium complex is the more active catalyst and atmospheric oxygen retards the catalytic activity by not allowing V(+5) to get reduced. Sluggish catalytic activity observed in the presence of atmospheric oxygen is, may be, due to the oxidising atmosphere created by it. Also, in the absence of TBAB no blue species was obtained indicating that bromide ion released from TBAB has active role in reducing the vanadium(+5) as is the only potent reductant present in the whole reaction mixture. Unfortunately, we have not been able to characterise the blue species X-ray crystallographically. However, after prolonged storage, block shaped yellow crystals were settled at the bottom of the vile containing blue reaction mixture collected after the catalytic reaction. This crystal was found to be the initial yellow catalyst **1**, however devoid of NH_4^+ ion that is thought to be eliminated during the reaction course.

Table 1. Cycloaddition of CO_2 to epoxide at room temperature using catalyst $NH_4[VO_2(Sal\text{-}ac)]$, **1**.

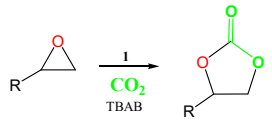

R: -CH_2Cl, -Ph

Entry	Epo-xide	[Epoxide]: **[Catalyst]**: [TBAB]	Time (h)	Temp (°C)	% Conver sion	Ref.
1	SO	100:**1**:2	2	60	86	Tw
2[a]	SO	100:**1**:2	2	60	77	Tw
3	ECH	100:**1**:2	14	45	99	Tw
4	SO	100:**1**:2	14	45	83	Tw
5	ECH	100:**1**:2	4	60	95	Tw
6	SO	100:**1**:2	4	60	91	Tw
7	SO	100:**0**:2	15	45	40	Tw
8	ECH	100:**1**:0	15	45	0	Tw
9[b]	SO	100:**0**:2	4	60	24	Tw
10	SO	100:**0**:2	4	60	37	Tw

View Article Online
DOI: 10.1039/C9NJ04606B

11[b]	SO	100:**1**:2	4	60	75	Tw
12[c]	SO	100:**1**:2	4	60	60	Tw

Reaction conditions: Unless mentioned reaction was done taking moistened TBAB and evacuating the atmospheric air from the reaction vessel with CO_2 gas; ECH = 1 mL (12.75 mmol); SO = 0.5 mL (4.3 mmol); $_pCO_2$ = 5 bar; 600 r.p.m. [a]Reaction was performed by taking catalyst **2**. [b]Unmoistened TBAB. [c]Reaction was done without flushing the atmospheric air from the reaction vessel with CO_2.

2.7 Study of blue reaction mixture

2.7.1 EPR Study

The EPR spectral measurement of the blue reaction mixture carried out at 298 K collected after the catalytic reaction reveals the presence of V(+4) center (Fig. 4). Thus, EPR spectroscopy supports the conversion of EPR silent V(+5) to EPR active V(+4) species.

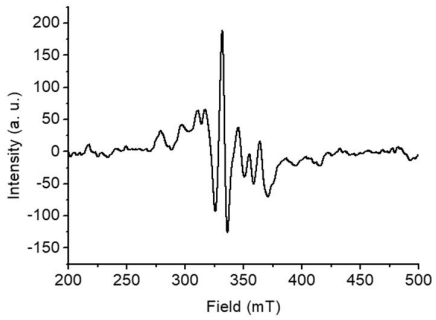

Fig. 4 X-band EPR spectrum in dimethyl sulfoxide (at 298 K) of the blue reaction mixture obtained after the catalytic reaction.

2.7.2 UV/Vis Spectroscopy

The UV/Vis studies were done by dissolving a portion of the blue reaction mixture in dimethyl sulfoxide (Fig. 5).

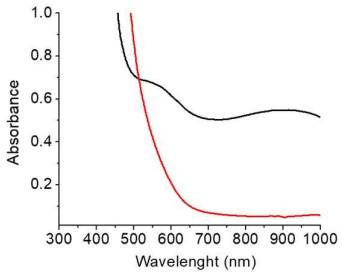

Fig. 5 UV/Vis spectrum of blue reaction mixture in DMSO (black line) and yellow solution obtained after addition of 3 drops of aqueous H_2O_2 solution to it (red line).

Two additional bands are observed in the spectra which are attributed to d-d transitions of V(+4). Also, the blue solution is indicative of vanadium (+4) oxidation state. To see the effect of oxidant, 3 drops of aqueous 30% solution of H_2O_2 was added to the blue reaction mixture which instantly changed to yellow. UV/Vis spectrum of this yellow solution shows the flattening of the peaks at 572 nm and 884 nm which were observed for the blue reaction mixture.[75] These changes in the UV/Vis spectrum indicates reoxidation to V(+5).

2.7.3 Crystallographic Characterization

Block shaped yellow crystals, settled at the bottom of the vile containing blue catalytic reaction mixture after its prolonged storage, was analysed by single crystal X-ray crystallography. These crystals assigned as complex **3**, although structurally identical with complex **2**, were actually generated from complex **1** upon elimination of NH_3 molecule from NH_4^+ ion which served as counter cation in complex **1**. A perspective view of complex **3** is illustrated in Fig. 6. Fig. S21† and Table S1 shows the crystal packing and data collection parameters, while selected bond distances and angles are tabulated in Table S2. The bond distances and angles of the crystal are very much similar with those of dioxo vanadium complexes.

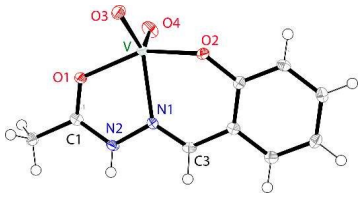

Fig. 6 A perspective view of **3** showing 50% thermal contours for all non-hydrogen atoms at 273(2) K obtained after the prolonged storage of the blue reaction mixture at open air. Selected bond distances (Å) and angles (°): for molecule **3**, V1-O1, 2.019(2); V1-O2, 1.879(2); V1-O3, 1.639(2); V1-O4, 1.614(2); V1-N1, 2.169(3); N1-N2, 1.386(3); N2-C1, 1.322(4); N1-C3, 1.300(4); O1-C1, 1.258(4); O(3)-V(1)-O(4), 109.23(13); O(1)-V(1)-O(2), 151.05(9).

2.7.4 ESI-mass Spectroscopy

The yellow product which is obtained from the blue catalytic reaction mixture after exposure to atmospheric air for long time is subjected to mass spectrometer and mass spectra (Fig. 7) reveals peaks at m/z, 261.0097 and m/z, 242.2854 which correspond to neutral dioxo vanadium catalyst and the TBAB cation, respectively. ESI-mass spectrum further reveals the elimination of NH_4^+ ion from the catalyst **1** during the reaction course.

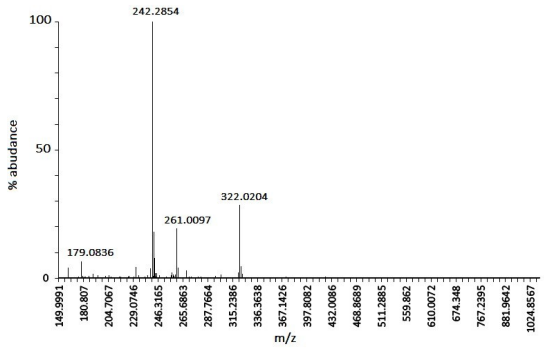

Fig. 7 ESI-mass spectrum of yellow product obtained from the blue catalytic reaction mixture.

DOI: 10.1039/C9NJ04606B

From the ESI MS and crystallographic evidence, it may be assumed that ligand coordination environment of the catalyst **1** is not completely destroyed during the catalytic reaction thereby helping in reformation of the dioxovanadium complex.

2.8 Catalytic Cycle

A plausible catalytic cycle is proposed in Scheme 2.

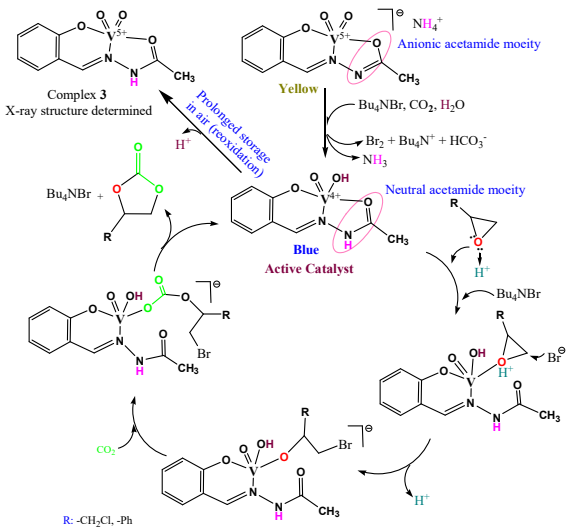

Scheme 2. Plausible catalytic cycle.

As mentioned earlier, bromide from TBAB acts as the reductant of V(+5) as it is the only reductant present in the reaction mixture. As per the crystal structure of the complex **3**, that crystallised out of the blue catalytic reaction mixture after its prolonged storage, the anionic acetamide moiety of the ligand is converted to the neutral acetamide moiety making the V-O bond weaker. Furthermore, reduction of V(+5) by bromide to V(+4) leads to less attraction of V(+4) center towards the O donor site of neutral acetamide moiety which will further weaken the V-O bond. As a result, neutral acetamide moiety will easily be detached from the metal center making available coordination site for the incoming epoxide substrate.[11] Moreover, the H^+, itself can act as activator of the epoxide.

3 Conclusion

In summary, two new dioxovanadium(+5) complexes **1** and **2** have been synthesised successfully and characterised with the help of X-ray crystallography, ^{1}H NMR, IR and UV/Vis spectroscopy. As complex **3** is unambiguously determined by X-ray crystallography, its further characterisation is not reported here as it is the same complex as **2**. Both complexes **1** and **2** exhibited efficient catalytic activity for the CO_2 addition to the epoxides, however complex **1** is more efficient than **2**. Catalytic reaction is enhanced in the presence of moisture. Interestingly, presence of atmospheric oxygen retards the catalytic capability of the complexes. During the catalytic process, vanadium (+5) complexes get reduced to +4 oxidation state which are evidenced by EPR and UV/Vis spectroscopy. This blue V(+4) complex is thought to be the more active *in situ* formed catalyst. The crystal structure of complex **3** obtained from the blue reaction mixture after prolonged storage might be greatly helpful in getting an insight into the mechanism of the catalytic reaction.

4 EXPERIMENTAL SECTION

4.1 Materials

All chemicals used in this work were purchased from Sigma Aldrich, Spectrochem and Alfa Aesar and were used without further purification.

4.2 Instrumentation

IR spectra were recorded on BRUKER infrared spectrometer (model no ALPHA II) using KBr. UV/Vis spectrum was taken on SHIMADZU spectrometer (model no UV-1800). ^{1}H NMR and ^{13}C NMR spectra were recorded on a Bruker 300 MHz spectrometer at 300 and 75 MHz, respectively with tetramethyl silane (TMS) as the internal standard. Solvents used were [D_6] DMSO, $CDCl_3$, and [D_4] methanol. Chemical shifts are reported in parts per million (δ), coupling constants (J values) are reported in Hertz (Hz) and spin multiplicities are indicated by the following symbols: s (singlet), d (doublet), t (triplet), m (multiplet), bs (broad singlet). The obtained data were expressed in delta (δ) parts per million. For taking mass spectroscopy WATERS-Q-Tof Premier-HAB213 was used. The thin layer chromatography (TLC) was performed with Merck pre-coated TLC plates. The column chromatography was performed using Merck silica gel (60-120 mesh).

Crystals of complex **1** and **2** were coated with light hydrocarbon oil and mounted at 296 K on the Bruker SMART APEX CCD diffractometer and intensity data were collected using graphite-monochromated Mo Kα radiation (λ= 0.71073 Å), whereas intensity data of complex **3** was collected at 273 K. The data integration and reduction were processed with SAINT software.[76] An absorption correction was applied.[77] Structures were solved by the direct method using SHELXS-2014/7 for complex **1** and **2** and SHELXT 2014/5 was used for complex **3.** Structure were refined on F^2 by full-matrix least-squares technique using the SHELXL-2014/7 program package[78] for complex **1** and **2** and SHELXL-2018/3 program package[79] was used for complex **3**. Non-hydrogen atoms were refined anisotropically. In the refinement, hydrogens were treated as riding atoms using SHELXL default parameters.

The X-band electron paramagnetic resonance (EPR) spectra were recorded on a JESFA200 ESR spectrometer, at room temperature with the experimental conditions [frequency, 9.449 GHz; power, 0.995 mW; field center, 490.00 mT, width, ± 500.00 mT; sweep time, 30.0 s; modulation frequency, 100.00 kHz, width, 0.1000 mT; amplitude, 100, and time constant, 0.03 s].

4.3 Syntheses of complexes

4.3.1 Synthesis of catalyst [NH_4][VO_2(Sal-ac)], 1. Ligand acetohydrazide was prepared by taking hydrazine hydrate (50 mmol) and ethyl acetate (50 mmol) in a 100 mL round bottom flask dissolved in a minimum volume of methanol. The reaction mixture

View Article Online
DOI: 10.1039/C9NJ04606B

was then refluxed for 5-6 hours with constant stirring. To this solution was added salicylaldehyde (50 mmol) slowly. Product immediately gets precipitated as light yellow solid which was filtered and then dried. The prepared N-salicylidenehydrazide ligand (300 mg, 1.68 mmol) and ammonium metavanadate (196.53 mg, 1.68 mmol) were taken in a round bottom flask and a minimum amount of methanol was added to get a clear solution. The contents were refluxed for 8-10 hours with constant stirring. The progress of the reaction was monitored in thin layer chromatography plate from time to time. After completion of the reaction, the methanol was distilled off under reduced pressure and the required product was obtained as yellow solid. This yielded **1** (350 mg, 75.2 %). UV/Vis λ_{max} (Methanol)/nm 219, 293 and 370. IR (KBr) ν_{max}/cm^{-1} 1614 (vs), 942 (vs) and 893 (vs). ^1H NMR δ_H (300 MHz, [D_6] DMSO) 8.71 (1H, s, HC=N), 7.47 (1H, m, Ar-H), 7.29 (1H, m, Ar-H), 7.11 (4H, s, NH_4^+), 6.73 (2H, m, Ar-H), 1.92 (3H, s, CH_3).

4.3.2 Synthesis of complex [VO_2(HSal-ac)], 2. The prepared N-salicylidenehydrazide (300 mg, 1.68 mmol) and ammonium metavanadate (196.53 mg, 1.68 mmol) were taken in a round bottom flasks and 5 mL of dimethyl formamide was added. The contents were heated at 80 °C for 5 hours. After completion of the reaction, the reaction mixture was kept overnight to obtain the product. Next batch of product was again collected by adding around 10 mL of toluene to the decanted solution of dimethylformamide. This yielded **2** (174.8 mg, 40 %). IR (KBr) ν_{max}/cm^{-1} 1601 (vs), 950 (vs), 893 (vs). ^1H NMR δ_H (300 MHz, [D_6] DMSO + 2 drops [D_4] methanol) 8.68 (1H,s,HC=N), 7.62 (1H, m, Ar-H), 7.45 (1H, m, Ar-H), 6.92 (1H, m, Ar-H), 6.82 (1H, m, Ar-H), 1.94 (3H, s, CH_3).

Conflicts of interest

"There are no conflicts to declare".

Acknowledgements

We thank DST-SERB, India, and CSIR, New Delhi, for financial support.

Notes and References

Crystal data for **1**: size 0.21 × 0.18 × 0.16 mm^3, orthorhombic, space group $P2_12_12_1$, Z = 4, a = 6.4268(4) Å, b = 13.3674(10) Å, c = 13.5577(10) Å, V = 1164.74(14) $Å^3$, Θ_{max} = 26°. R1 = 0.0241, wR2 (all data) = 0.0693. Goodness of fit on F2 = 1.059. CCDC 1876310 contains the supplementary crystallographic data of **1**.

Crystal data for **2**: size 0.35 × 0.22 × 0.19 mm^3, monoclinic, space group *P*21/n, Z = 4, a = 7.4612(9) Å, b = 11.9060(14) Å, c = 11.1849(13) Å, β = 99.077(7) °, V = 981.1(2) Å3, Θ_{max}= 26°. R1 = 0.0364, wR2 (all data) = 0.1088. Goodness of fit on F2 = 1.086. CCDC 1876310 contains the supplementary crystallographic data of **2**.

Crystal data for **3**: size 0.26 × 0.22 × 0.20 mm^3, monoclinic, space group *P*21/n, Z = 4, a = 7.3510(4) Å, b = 11.8967(7) Å, c = 11.1856(6) Å, β = 99.047(2) °, V = 966.04(9) $Å^3$, Θ_{max}= 26°. R1 = 0.0449, wR2 (all data) = 0.1039. Goodness of fit on F2 = 1.116. CCDC 1938067 contains the supplementary crystallographic data of **3**.

1. C. Calabrese, F. Giacalone and C. Aprile, *Catalysts*, 2019, **9**, 325.
2. M. S. Liu, X. Wang, Y. Jiang, J. Sun and M. Arai, *Catal. Rev.*, 2019, **61**, 214-269.
3. M. A. Gaona, F. de la. Cruz-Martínez, J. Fernández-Baeza, L. F. Sánchez-Barba, C. Alonso-Moreno, A. M. Rodríguez, A. Rodríguez-Diéguez, J. A. Castro-Osma, A. Otero and A. Lara-Sánchez, *Dalton Trans.*, 2019, **48**, 4218-4227.
4. G. N. Bondarenkoa, E. G. Dvurechenskayaa, O. G. Ganinaa, F. L. Alonsob and I. P. Beletskayaa, *Appl. Catal. B-Environ.*, 2019, **254**, 380-390.
5. S. Wanga and C. Xi, *Chem. Soc. Rev.*, 2019, **48**, 382.
6. Z. A. K. Khattaka, H. A. Younusa, N. Ahmada, B. Yud, H. Ullaha, S. Sulemana, A. H. Chughtaie, B. Moosavia, C. Somboona and F. Verpoorta, *J. CO_2 Util.*, 2018, **28**, 313-318.
7. C. Martín, G. Fiorani and A. W. Kleij, *ACS Catal.*, 2015, **5**, 1353−1370.
8. D. O. Meléndez, A. Lara-Sánchez, J. Martínez, X. Wu, A. Otero, J. A. Castro-Osma, M. North and R. S. Rojas, *ChemCatChem*, 2018, **10**, 2271-2277.
9. *S.* Kaneko and S. Shirakawa, *ACS Sustain. Chem. Eng.*, 2017, **5**, 2836-2840.
10. M. North, R. Pasquale and C. Young, *Green Chem.*, 2010, **12**, 1514–1539.
11. A. I. Elkurtehi and F. M. Kerton, *ChemSusChem*, 2017, **10**, 1249-1254.
12. C. Miceli, J. Rintjema, E. Martin, E. C. Escudero-Adán,C.Zonta, G. Licini and A. W. Kleij, *ACS Catal.*, 2017, **7**, 2367-2373.
13. Q. -W. Song, Z. -H. Zhoua and L. -N. He, *Green Chem.*, 2017, **19**, 3707-3728.
14. M. Aresta, A. Dibenedetto and A. Angelini, *Chem. Rev.*, 2014, **114**, 1709-1742.
15. I. Omae, *Coord. Chem. Rev.*, 2012, **256**, 1384-1405.
16. Q. Liu, L. Wu, R. Jackstell and M. Beller, *Nat. Commun.*, 2015, **6**, 5933.
17. A. J. Martín, G. O. Larrazábal and J. Pérez-Ramírez, *Green Chem.*, 2015, **17**, 5114-5130.
18. G. Fiorani, W. Guo and A. W. Kleij, *Green Chem.*, 2015, **17**, 1375-1389.
19. J. Klankermayer, S. Wesselbaum, K. Beydoun and W. Leitner, *Angew. Chem. Int. Ed.*, 2016, **55**, 7296-7343.
20. B. Yu and L. -N. He, *ChemSusChem*, 2015, **8**, 52-62.
21. A. Otto, T. Grube, S. Schiebahn and D. Stolten, *Energy Environ. Sci.*, 2015, **8**, 3283-3297.
22. C. Beattie and M. North, *RSC Adv.*, 2014, **4**, 31345-31352.
23. A. Coletti, C. J. Whiteoak, V. Conte and A. W. Kleij, *ChemCatChem*, 2012, **4**, 1190-1196.
24. N. Kielland, C. J. Whiteoak and A. W. Kleij, *Adv. Synth. Catal.*, 2013, **355**, 2115-2138.

DOI: 10.1039/C9NJ04606B

25. C. J. Whiteoak, N. Kielland,V. Laserna,E. C. Escudero-Adán, E. Martin and A. W. Kleij, *J. Am. Chem. Soc*., 2013, **135**, 1228−1231.
26. B. Schäffner, F. Schäffner, S. P. Verevkin and A. Börner, *Chem. Rev*., 2010, **110**, 4554−4581.
27. J. P. Vivek, N. Berry, G. Papageorgiou, R. J. Nichols and L. J. Hardwick, *J. Am. Chem. Soc*., 2016, **138**, 3745−3751.
28. K. Xu, *Chem. Rev*., 2004, **104**, 4303-4417.
29. M. Bahr and R. Mulhaupt, *Green Chem*., 2012, **14**, 483−489.
30. V. Besse, F. Camara, C. Voirin, R. Auvergne, S. Caillol and B. Boutevin, *Polym. Chem*., 2013, **4**, 4545−4561.
31. S. Fukuoka, M. Kawamura, K. Komiya, M. Tojo, H. Hachiya, K. Hasegawa, M. Aminaka, H. Okamoto, I. Fukawa and S. Konno, *Green Chem*., 2003, **5**, 497-507.
32. M. Fleischer, H. Blattmann and R. Mulhaupt, *Green Chem*., 2013, **15**, 934−94.
33. L. F. S. Souza, P. R. R. Ferreira, J. L. de Medeiros, R. M. B. Alve and O. Q. F. Araffljo, *ACS Sustain. Chem. Eng*., 2014, **2**, 62-69.
34. Z. Liu, P. R. Jensen and W. Fenical, *Phytochemistry*, 2003, **64**, 571-574.
35. S. Mizobuchi, J. Mochizuki, H. Soga, H. Tanba and H. Inoue, *J. Antibiot*. 1986, **39**, 1776-1778.
36. S. Chatterjee, G. C. Reddy, C. M. Franco, R. H. Rupp, B. N. Ganguli, H. W. Fehlhaber and H. Kogler, *J. Antibiot*., 1987, **40**, 1368-1374.
37. S. Naranga, R. Mehtab and S. N. Upadhyay, *Inorg. Nano-Met. Chem*., 2017, **47**, 909-916.
38. Y. Wang, Y. Qin, X. Wang and F. Wang, *Catal. Sci. Technol*., 2014, **4**, 3964-3972.
39. D. Tian, B. Liu, Q. Gan, H. Li and D. J. Darensbourg, *ACS Catal*., 2012, **2**, 2029-2035.
40. J. Meléndez, M. North and P. Villuendas, *Chem. Commun*., 2009, 2577-2579.
41. A. Decortes, A. M. Castilla and A. W. Kleij, *Angew. Chem. Int. Ed*., 2010, **49**, 9822–9837.
42. P. Li and Z. Cao, *Organometallics*, 2018, **37**, 406-414.
43. Y. Qin, H. Guo, X. Sheng, X. Wang and F. Wang, *Green Chem*., 2015, **17**, 2853-2858.
44. T. Ema, Y. Miyazaki, J. Shimonishi, C. Maeda and J. -Y. Hasegawa, *J. Am. Chem. Soc*., 2014, **136**, 15270-15279.
45. D. Bai, Z. Zhang, G. Wang and F. Ma, *Appl. Organometal. Chem*., 2015, **29**, 240–243.
46. Y. Ge, G. Cheng, N. Xu, W. Wang and H. Ke, *Catal. Sci. Technol*., 2019, **9**, 4255.
47. B. Ugale, S. Kumar, T. J. Dhilip Kumar and C. M. Nagaraja, *Inorg. Chem*., 2019, **58**, 3925-3936.
48. S. Huh, *Catalysts*,2019, **9**, 34.
49. B. Li, *Inorg. Chem. Commun*., 2018, **88**, 56-59.
50. W. Jiang, J. Yang, Y. -Y. Liu, S. -Y. Song and J. -F. Ma, *Chem. Eur. J*., 2016, **22**, 16991-16997.
51. C. Maeda, S. Sasaki, K. Takaishi and T. Ema, *Catal. Sci. Technol*., 2018, **8**, 4193-4198.
52. X. -F. Liua, Q. -W. Songa, S. Zhanga, L. -N. Hea, *Catal. Today*, 2016, **263**, 69-74.
53. G. Fiorani, W. Guoa and A. W. Kleij, *Green Chem*., 2015, **17**, 1375–1389
54. X. Wu, C. Chen, Z. Guo, M. North and A. C. Whitwood, *ACS Catal*., 2019, **9**, 1895-1906.
55. H. Q. Yang, X. Wang, Y. Ma, L. Wang and J. L. Zhang, *Catal. Sci. Technol*., 2016, **6**, 7773-7782.
56. D. J. Tao, F. F. Chen, Z. Q. Tian, K. Huang, S. M. Mahurin, D. E. Jiang and S. Dai, *Angew. Chem. Int. Ed*., 2017, **129**, 6947-6951.
57. Y. Ma, Y. Zhang, C. Chen, J. Zhang, B. Fan, T. Wang, T. Ren, L. Wang and J. Zhang, *Ind. Eng. Chem. Res*., 2018, **57**, 13342-13352.
58. W. Plass, *Coord. Chem. Rev*., 2003, **237**, 205-212.
59. S. Y. Ebrahimipour, I. Sheikhshoaie, J. Simpson, H. Ebrahimnejad, M. Dusek, N. Kharazmia and V. Eignerd, *New J. Chem.*, 2016, **40**, 2401.
60. K. H. Yang, *Acta Chim. Slov*., 2014, **61**, 629-636.
61. A. Pohlmann, S. Nica, T. Kim K. Luong and W. Plass, *Inorg. Chem. Commun.*, 2005, **8**, 289-292.
62. W. Plass and H. P. Yozgatli, *Z. Anorg. Allg. Chem*., 2003, **629**, 65-70.
63. D. Dragancea, N. Talmaci, S. Shova, G. Novitchi, D. Darvasiová, P. Rapta, M. Breza, M. Galanski, J. Kožíšěk, N. M. R. Martins, L. M. D. R. S. Martins, A. J. L. Pombeiro and V. B. Arion, *Inorg. Chem*., 2016, **55**, 9187-9203.
64. M. R. Maurya, S. Khurana, W. Zhang and D. J. Rehder, *J. Chem. Soc. Dalton Trans.,* 2002, 3015-3023.
65. H. H. Monfared, S. Kheirabadi, N. A. Lalami and P. Mayer, *Polyhedron*, 2011, **30**, 1375-1384.
66. M. Sutradhara, L. M. D. R. S. Martinsa, M. F. C. G. da Silva and A. J. L. Pombeiro, *Coord. Chem. Rev.*, 2015, **301-302**, 200-239.
67. M. Sutradhar and A. J. L. Pombeiro, *Coord. Chem. Rev.*, 2014, **265**, 89-124.
68. S. D. Kurbah, A. Kumar, I. Syiemlieh and R. A. Lal, *Inorg. Chem. Commun*., 2017, **86**, 6.
69. R. Dinda, P. K. Majhi, P. Sengupta, S. Pasayat, S. Ghosh, L. R. Favello and T. C. W. Mak, *Polyhedron*, 2010, **29**, 248.
70. A. Buchholz, S. Nica, R. Debel, A. Fenn, H. Breitzke, G. Buntkowsky and W. Plass, *Inorg. Chim. Acta.*, 2014, **166**, 420.
71. H. Hosseini-Monfared, N. Asghari-Lalami, A. Pazio, K. Wozniak and C. Janiak, *Inorg. Chim. Acta*., 2013, **406**, 241.
72. M. R. Maurya, C. Haldar, A. Kumar, M. L. Kuznetsov, F. Avecilla and J. C. Pessoa, *Dalton Trans*., 2013, **42**, 11941.
73. T. Bok, E. K. Noh and B. Y. Lee, *Bull. Korean Chem. Soc*., 2006, **27**, 1171-1174.
74. H. Li and Y. Niu, *Asian J. Chem.*, 2011, **23**, 3344-3346.
75. M. R. Maurya, B. Sarkar, F. Avecillab and I. Correia, *Dalton Trans*., 2016, **45**, 17343-17364.
76. G. M. Sheldrick, *SHELXL-2014, Program for Crystal Structure Refinement*, University of Göttingen, Göttingen, Germany, 2014.

View Article Online
DOI: 10.1039/C9NJ04606B

77. G. M. Sheldrick, *SHELXL-2018*: Program for Crystal Structure Refinement, University of Göttingen, Göttingen, Germany, 2018.
78. *SAINT+*, 6.02 ed.; Bruker AXS, Madison, WI, 1999.
79. G. M. Sheldrick, SADABS 2.0, 2000.

View Article Online
DOI: 10.1039/C9NJ04606B

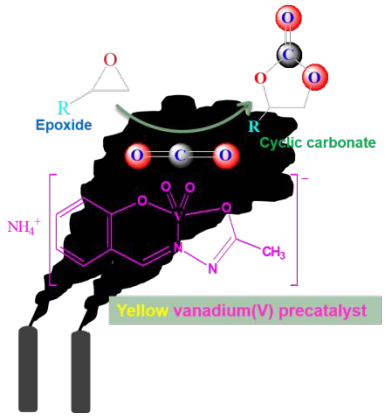

***In situ* formed vanadium(+4) species catalyzed** carbon dioxide fixation reaction leading upto 99 % conversion of epoxides to cyclic carbonates under mild condition is reported here along with study on the ***in situ* formed catalyst** to some extent.